



Contents lists available at ScienceDirect

Electrochemistry Communications

journal homepage: www.elsevier.com/locate/elecom

Thermal stabilities of delithiated olivine MPO_4 ($M = Fe, Mn$) cathodes investigated using first principles calculations

Shyue Ping Ong, Anubhav Jain, Geoffroy Hautier, Byoungwoo Kang, Gerbrand Ceder*

Department of Materials Science and Engineering, Massachusetts Institute of Technology, 77 Massachusetts Ave, Cambridge, MA 02139, USA

ARTICLE INFO

Article history:

Received 6 December 2009

Received in revised form 29 December 2009

Accepted 6 January 2010

Available online xxxxx

Keywords:

Thermal stability

Olivine

Cathode

 $LiMnPO_4$ $LiFePO_4$ $MnPO_4$ $FePO_4$

Density functional theory

Phase diagrams

ABSTRACT

We present an analysis of the thermal reduction of delithiated $LiMnPO_4$ and $LiFePO_4$ based on the quaternary phase diagrams as calculated from first principles. Our results confirm the recent experimental findings that $MnPO_4$ decomposes at a much lower temperature than $FePO_4$, thereby potentially posing larger safety issues for $LiMnPO_4$ cathodes. We find that while substantial oxygen is released as $MnPO_4$ reduces to $Mn_2P_2O_7$, the mixed valence phases that form in the decomposition process of $FePO_4$ limit the amount of oxygen evolved.

© 2010 Elsevier B.V. All rights reserved.

1. Introduction

The olivine $LiMPO_4$ materials ($M = Fe, Mn, Ni, Co$) form a promising class of cathode materials for rechargeable Li batteries. $LiFePO_4$ [1], in particular, has already found widespread applications in industry due to its reasonable theoretical capacity of 170 mA h g^{-1} , low cost and low toxicity. In recent years, there has been increasing interest in $LiMnPO_4$, $LiCoPO_4$ and $LiNiPO_4$ which could potentially deliver higher theoretical energy densities than $LiFePO_4$ due to their higher measured/predicted voltages of 4.1 V, 4.8 V and 5.1 V versus Li/Li^+ , respectively [2–4].

Of these promising alternatives, $LiMnPO_4$ has garnered the most interest because its voltage of 4.1 V is higher than $LiFePO_4$ (3.5 V) but well within the limitations of current organic electrolytes. While focus has been on understanding $LiMnPO_4$'s poor rate performance due to low ionic and electronic conductivities [5], a high surface energy barrier for Li diffusion [6], or significant volume change at the phase boundary [7–9], it has been tacitly assumed that the charged compound, $MnPO_4$, would match the excellent thermal stability of $FePO_4$, which is a major contribution to Li-ion battery safety. Two recent investigations by Kim et al. [10]

and Chen et al. [11] have cast doubt on that assumption by demonstrating that while fully lithiated $LiMnPO_4$ remains stable up to fairly high temperatures, delithiated $MnPO_4$ decomposes at temperatures of around 150–200 °C, evolving O_2 and heat in the process. This is in stark contrast to delithiated $FePO_4$ which has been shown to be stable for temperatures up to 500–600 °C [12].

In this work, we constructed the oxygen grand potential phase diagrams for the $Li-M-P-O$ ($M = Fe, Mn$) systems using the methodology developed in our previous work [13]. We were able to confirm the lower stability of $MnPO_4$, and demonstrate that the difference in the relative stabilities of the delithiated MPO_4 phases can be explained in terms of the competing phases present in the phase diagrams.

2. Methodology

2.1. Thermodynamic methodology

In our previous work [13], we outlined a thermodynamic methodology in which oxygen grand potential phase diagrams can be constructed from first principles. Interested readers are referred to that paper for further details. Such phase diagrams represent phase equilibria in an isothermal, isobaric system that is open with respect to oxygen, which is representative of conditions during synthesis and operation of $LiMPO_4$ cathodes.

* Corresponding author. Tel.: +1 617 253 1581; fax: +1 617 258 6534.

E-mail addresses: shyue@mit.edu (S.P. Ong), anubhavj@mit.edu (A. Jain), hautier@mit.edu (G. Hautier), bwkang@mit.edu (B. Kang), gceder@mit.edu (G. Ceder).

In the open Li–M–P–O system at temperatures of interest (≈ 200 – 1000 K), most phase equilibria changes are solid-state reactions involving the absorption or loss of oxygen. We may therefore make the simplifying assumption that the reaction entropy is dominated by the oxygen entropy. The effect of temperature and partial pressure is mostly captured by changes in the oxygen chemical potential, as follows:

$$\mu_{\text{O}_2}(T, p_{\text{O}_2}) = \mu_{\text{O}_2}(T, p_0) + kT \ln \frac{p_{\text{O}_2}}{p_0} \quad (1)$$

$$= E_{\text{O}_2} + kT - TS_{\text{O}_2}^{T, p_0} + kT \ln \frac{p_{\text{O}_2}}{p_0} \quad (2)$$

where p_{O_2} is the oxygen partial pressure, p_0 is a reference oxygen partial pressure, $S_{\text{O}_2}^{T, p_0}$ is the oxygen entropy, E_{O_2} is the oxygen energy, and k is Boltzmann's constant. Eq. (2) is obtained by writing the chemical potential as a Legendre transform of the internal energy, with an ideal gas assumption made for the PV term.

Lowering μ_{O_2} corresponds to more reducing environments brought about by higher temperatures, lower oxygen partial pressures or the presence of reducing agents. In this work, we have set the reference oxygen chemical potential to be zero at the room temperature air (298 K, 0.21 atm) value obtained with the calculated value of E_{O_2} in Eq. (2). This calculated value has been shifted by -1.36 eV to correct for the O_2 binding energy error and GGA error associated with adding electrons to the oxygen p orbital when O^{2-} is formed. Experimental entropy data for O_2 at 0.1 MPa were obtained from the JANAF thermochemical tables [15].

2.2. Computational methodology

We calculated the energies of all structural prototypes in the Li–Fe–P–O and Li–Mn–P–O systems in the 2006 version of the Inorganic Crystal Structure Database [16] for both the Fe and Mn compositions. Compounds having partial occupancies were related to the ordered structure with lowest electrostatic energy [17,18] at the same or close composition from a group of representative structures enumerated with a technique similar to that proposed by Hart and Forcade [19].

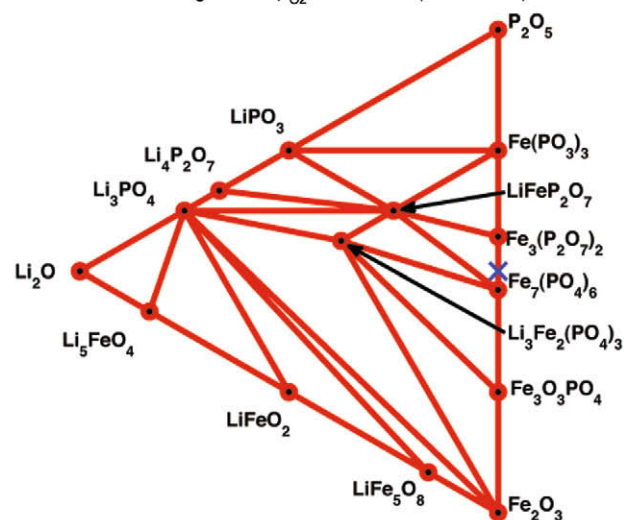
All energies were calculated using the Vienna ab initio simulation package [20] within the projector augmented-wave approach [21], using the Perdew–Burke–Ernzerhof generalized-gradient functional [22] and the GGA+U extension to it [23]. $U_{\text{effective}}$ values of 3.9 eV and 4.0 eV were used for Mn and Fe, respectively, following Wang's method [14] of fitting the calculated binary oxide formation enthalpies to experimental values from the Kubachewski tables [24]. A plane wave energy cut-off of 520 eV and k -point density of at least 500/(number of atoms in unit cell) were used for all computations. All calculations were spin-polarized starting from a high-spin ferromagnetic configuration for Fe and Mn.

3. Results

3.1. Phase diagrams at critical μ_{O_2} for reduction

To investigate the stability of delithiated MnPO_4 and FePO_4 , we have constructed the phase diagrams at various μ_{O_2} . Increased temperature leads to a more reducing condition, i.e. more negative μ_{O_2} . Hence, the critical temperature for reduction of MPO_4 corresponds to an μ_{O_2} below which the compound decomposes. The equilibrium reduction products are then given by the phases stable below this critical μ_{O_2} . Fig. 1 shows the oxygen grand potential phase diagrams for the Li–Fe–P–O and Li–Mn–P–O systems at μ_{O_2} just below that required for the reduction of the delithiated olivine MPO_4 phase. It should be noted that the delithiated olivine

(a) Li–Fe–P–O Phase Diagram at $\mu_{\text{O}_2} = -1.72$ eV ($T \approx 700^\circ\text{C}$)



(b) Li–Mn–P–O Phase Diagram at $\mu_{\text{O}_2} = -0.83$ eV ($T \approx 370^\circ\text{C}$)

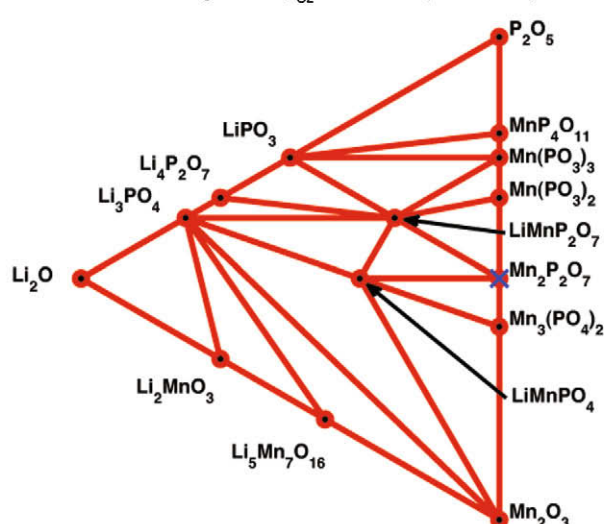
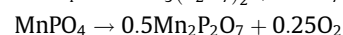
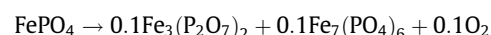


Fig. 1. Li–M–P–O phase diagrams for μ_{O_2} just below critical values where delithiated MPO_4 olivine decomposes. The composition of MPO_4 is marked with an X.

is not the ground state structure for the FePO_4 composition, and the trigonal ground state phase and all phases lower in energy than the olivine phase [25] have been removed from the dataset to determine the non-equilibrium reduction pathway. We will discuss the consequence of this removal in the next section.

Reduction of FePO_4 takes place at a much lower μ_{O_2} of -1.72 eV ($\approx 700^\circ\text{C}$ under air) compared to MnPO_4 which reduces at μ_{O_2} of -0.83 eV ($\approx 370^\circ\text{C}$). From the phase triangle bounding the MPO_4 compositions, we determine that FePO_4 and MnPO_4 undergo the following initial reduction reactions:



The predicted reduction temperatures and products are in fairly good agreement with experimental findings. Delacourt et al. [12] have previously reported the formation of the mixed valence $\text{Fe}_7(\text{PO}_4)_6$ phase for Li_xFePO_4 ($x < 1$) at 500 – 600°C . Kim et al. [10] and Chen and Richardson [11] also reported that the decomposition of MnPO_4 leads to the formation of $\text{Mn}_2\text{P}_2\text{O}_7$ at 150 – 200°C . The

calculated temperatures may differ from experimentally measured temperatures for several reasons. Firstly, a 100 K temperature difference corresponds to about 10 meV, well within the errors of our DFT calculations and entropy approximations (refer to our previous work [13] for a more detailed discussion). Secondly, the presence of reducing agents such as the electrolyte and carbon under experimental conditions will tend to decrease the actual decomposition temperatures. We also observe that in MnPO_4 decomposition, the Mn/P ratio stays constant and only O_2 release takes place, while for FePO_4 , longer range transport will be needed to create phases with Fe/P ratio different from 1.

3.2. O_2 evolved versus temperature

Fig. 2 summarizes the O_2 evolution versus temperature for the reduction paths of FePO_4 and MnPO_4 . Both the non-equilibrium paths and the equilibrium paths are shown for FePO_4 . The non-equilibrium path corresponds to the likely reaction path if the FePO_4 olivine is unable to transform to the lowest energy trigonal structure [26,27] (space group $P3_121$) due to kinetic limitations, and proceeds to reduce into other phases with the evolution of oxygen. The equilibrium path assumes that olivine FePO_4 is able to transform first into the trigonal phase before undergoing reduction.

For FePO_4 , O_2 evolution takes places at a much lower temperature for the non-equilibrium path as compared to the equilibrium path. The path taken depends on the relative kinetics, which is affected by experimental conditions and Li content. Stability investigations by Yang et al. [27] and Rouse et al. [27] have shown that orthorhombic FePO_4 transforms irreversibly to trigonal FePO_4 only at fairly high temperatures of 600–700 °C, though there is some controversy as to the transition temperature for this structural transformation [25]. Regardless, the fact that the mixed valence $\text{Fe}_7(\text{PO}_4)_6$ was observed by Delacourt et al. [12] during Li_xFePO_4 ($x \ll 1$) decomposition at 500–600 °C suggests that at least some degree of non-equilibrium decomposition does take place under certain experimental conditions. For MnPO_4 , the olivine phase is the lowest energy structure. Nonetheless, the critical temperature for the onset of O_2 evolution in non-equilibrium FePO_4 reduction is still much higher than that for MnPO_4 .

From Fig. 2, we may also observe that initial reduction of FePO_4 evolves 0.1 moles of oxygen per mole of cathode, compared to 0.25 moles for initial reduction of MnPO_4 . Hence, not only does MnPO_4 reduce at a much lower temperature than FePO_4 , it also evolves 2.5 times the amount of O_2 . Even at higher temperatures between 1100 °C and 1300 °C, FePO_4 only evolves 0.17 moles of oxygen

per mole of cathode, significantly less than MnPO_4 . This greater amount of O_2 evolved for MnPO_4 presents a significant safety hazard as O_2 released can ignite the organic electrolytes used in rechargeable Li batteries.

4. Discussion

Our results show that delithiated FePO_4 is inherently more thermally stable than MnPO_4 , and the amount of O_2 evolved upon initial decomposition is also much less. The greater stability of FePO_4 over MnPO_4 may be explained through ligand field theory [28]. It is well-known that in an octahedral environment such as MO_6 in olivines, half-filled high-spin $t_{2g}^3 e_g^2$ is a highly stable electronic configuration due to the exchange stabilization arising from the five parallel-spin electrons. We would therefore expect that Fe^{3+} and Mn^{2+} , both of which have the high-spin $t_{2g}^3 e_g^2$ half-filled configuration, to have greater stability as compared to Fe^{2+} and Mn^{3+} respectively. Indeed, there is a greater proportion of Mn^{2+} phases relative to Mn^{3+} in the Li–Mn–P–O phase diagram, whereas the situation is reversed in the case of Fe. Furthermore, LiMnPO_4 is stable over a much wider range of oxygen chemical potentials ($-0.56 \text{ eV} < \mu_{\text{O}_2} < -7.02 \text{ eV}$) than LiFePO_4 ($-2.36 \text{ eV} < \mu_{\text{O}_2} < -6.24 \text{ eV}$). A similar argument has been used to explain why the LiFePO_4 voltage is unusually low [2].

The key factor influencing the amount of O_2 evolved is the competing phases present in the system, which is also related to the relative stabilities of the +2 and +3 oxidation states. In the Fe system, the relative stability of the Fe^{3+} oxidation state leads to the presence of the mixed valence $\text{Fe}_7(\text{PO}_4)_6$ and $\text{Fe}_3(\text{P}_2\text{O}_7)_2$ phases, which results in a smaller amount of O_2 evolved. On the other hand, MnPO_4 immediately reduces to $\text{Mn}_2\text{P}_2\text{O}_7$ which has the Mn^{2+} oxidation state, resulting in significantly higher O_2 evolution.

Huggins [29] has previously performed a thermodynamic analysis of the relationship between equilibrium Li voltages and oxygen partial pressure for a number of ternary oxide systems. He found that extrapolation of the observed trends indicates high values of equilibrium O_2 partial pressures in high voltage materials. Our results similarly suggest that there could be some tradeoff between higher voltage and thermal stability of the charged cathode. However, the voltage of a rechargeable Li battery cathode material is related to the difference in energies between the delithiated and lithiated phases [2]. Therefore, a higher voltage can come from either a more stable lithiated phase, or a less stable delithiated phase. So this tradeoff between higher voltage and thermal stability of the charged cathode may not be absolute. We also note that coating strategies have been successfully employed to stabilize the charged cathode in LiCoO_2 batteries [30,31], and similar strategies could possibly be developed for the olivine cathodes to mitigate safety concerns.

5. Conclusion

In this work, we have analyzed the thermal stabilities of delithiated FePO_4 and MnPO_4 by constructing the oxygen grand potential phase diagrams of the Li–M–P–O ($M = \text{Fe}, \text{Mn}$) systems using first principles calculations. Our observations indicate, in agreement with recent experiment findings [10,11], that MnPO_4 reduces with substantial oxygen release at a much lower temperature than FePO_4 . Hence, the Mn system may trade off its somewhat higher energy density with considerably lower safety. The difference in relative stabilities of FePO_4 and MnPO_4 may be explained by the competing phases present in the phase diagrams and relative stabilities of the M^{2+} and M^{3+} as explained by ligand field theory. The technique outlined in this paper can conceivably be extended to other similar systems, e.g. Li–Co–P–O and Li–Ni–P–O.

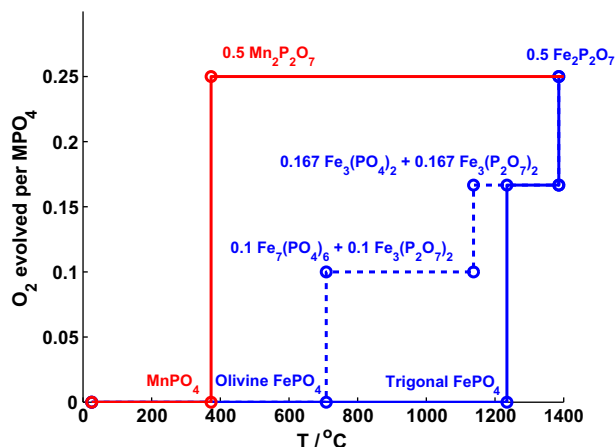


Fig. 2. O_2 evolved versus temperature for delithiated MPO_4 ($M = \text{Fe}, \text{Mn}$).

Acknowledgements

This work was supported by the BATT Program under Contract DE-AC02-05CH11231, the US Department of Energy under Contract No. DE-FG02-05ER46253 and DE-FG02-97ER25308, and the NSF under Grant No. DMR-0606276. We would also like to thank the Robert Bosch Company and Umicore for their support, and Chris Fischer, Tim Mueller, and Charles Moore for their assistance in the development of the high-throughput battery screening environment.

References

- [1] A. Padhi, K. Nanjundaswamy, J. Goodenough, *J. Electrochem. Soc.* 144 (1997) 1188–1194.
- [2] F. Zhou, M. Cococcioni, K. Kang, G. Ceder, *Electrochem. Commun.* 6 (2004) 1144–1148.
- [3] G. Li, H. Azuma, M. Tohda, *Electrochem. Solid-State Lett.* 5 (2002) A135.
- [4] K. Amine, H. Yasuda, M. Yamachi, *In Situ* 3 (2000) 178–179.
- [5] C. Delacourt, L. Laffont, R. Bouchet, C. Wurm, J.-B. Leriche, M. Morcrette, J.-M. Tarascon, C. Masquelier, *J. Electrochem. Soc.* 152 (2005) A913.
- [6] L. Wang, F. Zhou, G. Ceder, *Electrochem. Solid-State Lett.* 11 (2008) A94.
- [7] A. Yamada, S.-C. Chung, *J. Electrochem. Soc.* 148 (2001) A960.
- [8] A. Yamada, Y. Kudo, K.-Y. Liu, *J. Electrochem. Soc.* 148 (2001) A1153.
- [9] N. Meethong, H.-Y. Huang, S. Speakman, W. Carter, Y.-M. Chiang, *Adv. Funct. Mater.* 17 (2007) 1115–1123.
- [10] S.-W. Kim, J. Kim, H. Gwon, K. Kang, *J. Electrochem. Soc.* 156 (2009) A635.
- [11] G. Chen, T.J. Richardson, *J. Power Sources* 195 (2010) 1221–1224.
- [12] C. Delacourt, P. Poizot, J.-M. Tarascon, C. Masquelier, *Nat. Mater.* 4 (2005) 254–260.
- [13] S. Ong, L. Wang, B. Kang, G. Ceder, *Chem. Mater.* 20 (2008) 1798–1807.
- [14] L. Wang, T. Maxisch, G. Ceder, *Phys. Rev. B* 73 (2006) 1–6.
- [15] M.W. Chase, *NIST-JANAF Thermochemical Tables*, vol. 12, American Chemical Society, New York, 1998.
- [16] G. Bergerhoff, R. Hundt, R. Sievers, I.D. Brown, *J. Chem. Inform. Comput. Sci.* 23 (1983) 66–69.
- [17] P.P. Ewald, *Annalen der Physik* 64 (1921) 253–287.
- [18] A. Toukmaji, J.A. Board, *Comput. Phys. Commun.* 95 (1996) 73–92.
- [19] G.L.W. Hart, R.W. Forcade, *Phys. Rev. B* 77 (2008) 1–12.
- [20] G. Kresse, J. Furthmuller, *Phys. Rev. B* 54 (1996) 11169–11186.
- [21] P.E. Blochl, *Phys. Rev. B* 50 (1994) 17953–17979.
- [22] J.P. Perdew, M. Ernzerhof, K. Burke, *J. Chem. Phys.* 105 (1996) 9982.
- [23] V.I. Anisimov, F. Aryasetiawan, A.I. Lichtenstein, *J. Phys.: Condens. Matter* 9 (1997) 767–808.
- [24] O. Kubaschewski, C.B. Alcock, P.J. Spencer, *Thermochemical Data*, Pergamon Press, 1993 (Chapter 5).
- [25] M.E. Arroyo, Y. De Dompablo, N. Biskup, J.M. Gallardo-Amores, E. Moran, H. Ehrenberg, U. Amador, *Chem. Mater.* 8 (2009) 091109144106046.
- [26] S. Yang, Y. Song, P.Y. Zavalij, M.S. Whittingham, *Electrochem. Commun.* 4 (2002) 239–244.
- [27] G. Rousse, J. Rodriguez-Carvajal, S. Patoux, C. Masquelier, *Chem. Mater.* 131 (2003) 4082–4090.
- [28] H.L. Schläfer, G. Gliemann, *Basic Principles of Ligand Field Theory*, Wiley-Interscience, New York, 1969.
- [29] R.A. Huggins, *ECS Trans.* 16 (2009) 37–47.
- [30] J. Cho, *Electrochim. Acta* 48 (2003) 2807–2811.
- [31] A.T. Appapillai, A.N. Mansour, J. Cho, Y. Shao-Horn, *Chem. Mater.* 19 (2007) 5748–5757.